Finite-Bandwidth Effects in One-Dimensional Wigner Lattices

De Raedt, H.; Lagendijk, A.

Published in:
Physical Review. B, Condensed Matter

DOI:
10.1103/PhysRevB.27.921

Finite-bandwidth effects in one-dimensional Wigner lattices

Hans De Raedt
Physics Department, University of Antwerp, Universiteitsplein 1, B-2610 Wilrijk, Belgium

Ad Lagendijk
Natuurkundig Laboratorium, University of Amsterdam, Valckenierstraat 65, 1018 XE, The Netherlands
(Received 19 May 1982)

The Feynman path-integral formalism is used to calculate the thermodynamic properties of a one-dimensional (1D) spinless fermion model with nearest- and next-nearest-neighbor interaction. The mapping of this 1D quantum model on a two-dimensional classical model allows the use of a Monte Carlo method to calculate the properties of long chains. We present results for typical values of the interaction parameters, density, and temperature. We find that a finite bandwidth smears out the details of the classical ground-state configurations discussed by Hubbard. If the density $\rho \neq \frac{1}{2}$, we find that the static structure factor and the static susceptibility display a maximum at $2k_F$ only when the next-nearest-neighbor interaction is nonzero.

I. INTRODUCTION

Recently, Hubbard[1] derived the ground state of the one-dimensional (1D) spinless fermion lattice model

$$H=-t\sum_{i=1}^{M}(c_i^{\dagger}c_{i+1}+c_{i+1}^{\dagger}c_i)+\tfrac{1}{2}\sum_{i\neq j}^{M}V(|i-j|)c_i^{\dagger}c_i c_j^{\dagger}c_j\ , \tag{1.1}$$

in the zero-bandwidth limit $t=0$. He showed that under certain restrictions on the interaction $V(l)\equiv V_l$, the ground state is periodic. The period as well as the arrangement of the particles within each period depend on the particle density $\rho=N/M$. These ground-state configurations may be regarded as generalized one-dimensional classical Wigner lattices.[1] According to Hubbard, this classical model might offer a possible explanation for the optical spectra of tetracyanoquinodimethane (TCNQ) salts and the satellites in x-ray diffraction. As pointed out by Hubbard, it is not clear whether his conclusions remain valid if the finite bandwidth is taken into account.

The purpose of this paper is to investigate the effect of a finite bandwidth in more detail. To demonstrate that it is possible to calculate the properties of (1.1), we will assume that $V(3)=V(4)=\cdots=0$. We will use the Monte Carlo method used previously by us[2] for the case $V(2)=V(3)=\cdots=0$ as a computational tool. In contrast to Monte Carlo methods based on a local decomposition of the Hamiltonian (1.1),[3,4] it is very simple to include these more-distant interactions in our approach.

Detailed information about the arrangement of the particles can be extracted from the static structure factor and the static susceptibility

$$S(q)=\langle\rho_q\rho_{-q}\rangle-\delta_{q,0}\langle\rho_q\rangle^2\ , \tag{1.2}$$

$$\chi(q)=\int_0^{\beta}d\lambda\,\langle e^{\lambda H}\rho_q e^{-\lambda H}\rho_{-q}\rangle-\beta\delta_{q,0}\langle\rho_q\rangle^2\ , \tag{1.3}$$

where ρ_q is the Fourier transformed density and β denotes the inverse temperature. The static structure factor measures the density fluctuations, and the static susceptibility is the linear response of the density to an external field. We will calculate $S(q)$ and $\chi(q)$ for several sets of parameters β, ρ, $V(1)$, and $V(2)$. To get an idea of the behavior of $S(q)$ and $\chi(q)$, it is instructive to consider special cases for which analytic results are known. Because these special cases are very useful for the interpretation of the simulation data, we summarize those features which are relevant to our discussion.

The most simple case is the free-fermion limit $t\neq 0$, $V(1)=V(2)=0$. The zero-temperature results for $S(q)$ and $\chi(q)$ are

$$S(q)=\rho-(\rho-q/2\pi)\Theta(2k_F-|q|)\ , \tag{1.4}$$

$$\chi(q)=\frac{1}{4\pi t\sin(q/2)}\ln\left|\frac{\sin(q/2)+\sin k_F}{\sin(q/2)-\sin k_F}\right|\ , \tag{1.5}$$

where $k_F=\pi\rho$ denotes the Fermi wave vector. Note that $S(q)=\rho$ if $2k_F<q<2(\pi-k_F)$, and that the susceptibility (1.5) has a logarithmic divergency at $|q|=2k_F$. Treating the interacting system in the Hartree-Fock approximation yields expressions for $S(q)$ and $\chi(q)$ which have the same functional dependence on k_F and q as the free-fermion model has. Except at low densities, the mean-field result (1.4) is in qualitative disagreement with previous simulation data.[2]

The case $V(1)\neq 0$ and $V(2)=0$ has been studied in great detail. The Jordan-Wigner transformation is used to write the Hamiltonian (1.1) as a spin-$\frac{1}{2}$ Ising-Heisenberg chain. The Bethe ansatz and the correspondence with this X-X-Z Hamiltonian can then be exploited to analyze the ground state, the low-lying excitations, and the thermodynamic functions.[5-7] At $T=0$, $\rho\neq\frac{1}{2}$ the system is always metallic,[5] but for $T=0$, $\rho=\frac{1}{2}$ there is a metal-insulator transition at $V(1)=2t$ and there are long-range density correlations unless $V(1)<2t$.

The classical limit is obtained by putting $t=0$. The ground-state configurations for $V(1)>2V(2)$ and arbitrary ρ are given by Hubbard's algorithm.[1] For $\rho=\frac{1}{2}$, this model is equivalent to a 1D Ising model in an external field. The ground state is $|10101010\cdots\rangle$ if $V(1)>2V(2)$ or $|11001100\cdots\rangle$ if $V(1)<2V(2)$. In the former case $S(q)$ and $\chi(q)$ diverge at $q=\pi$, while in the latter divergencies are at $q=\pi/2$ and $q=3\pi/2$. At nonzero temperatures, the classical Monte Carlo method can be used to study the model properties.[8]

II. COMPUTATION

As already mentioned in the Introduction, we will apply a Monte Carlo method for fermion systems to study the thermodynamics of the quantum model (1.1). Here we will only discuss some aspects of our method which are relevant to the interpretation of the data. A more detailed description can be found in Ref. 2.

The starting point in the formulation of a Monte Carlo approach to quantum statistical mechanics is the Trotter formula[9]

$$Z\equiv \mathrm{Tr}e^{-\beta H}=\lim_{m\to\infty} Z_m \ , \tag{2.1a}$$

$$Z_m=\mathrm{Tr}(e^{-\tau H_0}e^{-\tau H_1})^m \ . \tag{2.1b}$$

Here H_0 represents the free-fermion Hamiltonian, $H_1=H-H_0$, and $\tau=\beta/m$. If we insert resolutions of the identity between the exponential operators in (2.1b), we obtain a discrete version of the Feynman path integral of a fermion system.[2,10] For m fixed, we may interpret Z_m in terms of a 2D classical model, m playing the role of an extra dimension. The actual value of m depends on β, ρ, and the lattice size M. The basic idea of the method is to calculate the properties of the quasiclassical model defined by (2.1b) and to study the convergence of the results as a function of m.[2]

In this paper we present data for a ring of 32 sites and temperatures down to $T=0.5$ (we put $t=1$). The choice of a 32-site lattice is a compromise between computation time and possible values of ρ. We now argue that for the interacting system $T=0.5$ corresponds to low temperature. We present our arguments for $\rho=\frac{1}{2}$ because in this case quantum fluctuations are the most important. As pointed out in Ref. 2, the fermion properties are calculated by simulating the boson model

$$H=-t\sum_{i=1}^{M}(b_i^\dagger b_{i+1}+b_{i+1}^\dagger b_i)+\tfrac{1}{2}\sum_{i\neq j}^{M}V(|i-j|)b_i^\dagger b_i b_j^\dagger b_j+\cdots \ , \tag{2.2}$$

where the ellipsis stands for a hard-core potential. This potential prevents two particles from occupying the same site. This Hamiltonian can be shown to be equivalent to the X-X-Z spin-$\frac{1}{2}$ model and is also related to the large-U limit of the extended Hubbard model.[11] Thus we can compare the ground-state energy of the spin model[12] with the thermal energy obtained from (2.2). In the Heisenberg limit, $V(1)=2t$ and $V(2)=0$, we have

$$E_0^{\mathrm{boson}}=E_0^{\mathrm{spin}}+\tfrac{1}{2}=-0.38629 \ , \tag{2.3a}$$

whereas the simulation result for $\beta=2$, $m=32$ is

$$E^{\mathrm{boson}}=-0.398\pm 0.009 \ . \tag{2.3b}$$

Thus it is reasonable to assume that $\beta=2$ corresponds to low temperature.

We close this section by summarizing some technical details of the simulation. To check our program we first reproduced the exact results for one, two, three, and four particles on eight sites for several values of β, m, $V(1)$, and $V(2)$. In our opinion this should always be done first. Any Monte Carlo method that fails to pass this simple but essential test cannot be relied upon. Because the computation time increases as m increases, the optimum value of m is the minimum value of m for which the difference between the exact results, and

the calculated results are less than the statistical errors.[2] In our final simulations, $1000mN$ single-particle steps (1000 lattice sweeps) were discarded before taking samples. Most of the data presented here have been obtained by averaging three runs of 20 000 samples each. The number of single-particle steps between two successive samples is mM. Occasionally, runs of 300 000 samples have been made to assure that there were no systematic errors. We also checked that the choice of the start configuration had a negligible effect on the results. The statistical errors are less than 5%. Comparing the data with results of several runs for a ring of 64 sites, we conclude that finite-size effects are smaller than the statistical errors. In general, the statistical errors on the boson data are much smaller than that on the fermion data. We observe that the main source of statistical fluctuations comes from quantities related to the kinetic energy H_0. This could be expected because we are simulating a quantum-mechanical model in real space instead of in momentum space. The computation time strongly depends on the number of different quantities one wants to calculate. For instance, we were forced to estimate $\chi(q)$ with less statistical precision than $S(q)$ (see the Appendix). The longest run ($\beta=2$, $M=32$, $m=32$, $\rho=\frac{1}{2}$) took 3 h of CPU (central processing unit) time on a Digital Equipment Corporation VAX-11/780 computer.

III. RESULTS

We first demonstrate that our simulation data is in agreement with the behavior expected in the special case $V(2)=0$.[5,6,11] In Fig. 1 we depict $S(q)$ at intermediate temperature in the case of a half-filled band and $V(2)=0$. The maximum of $S(q)$ grows rapidly as $V(1)$ becomes larger than 2, as can be inferred from the equivalence with the X-X-Z model.[5,6] A comparison between $\beta S(q)$ and $\chi(q)$ in the "Heisenberg limit" [$V(1)=2$, $V(2)=0$, $\rho=\frac{1}{2}$] is given in Fig. 2. It demonstrates that the Bogoliubov inequality $\chi(q)\leq\beta S(q)$ is satisfied by our approximate expression of $\chi(q)$ derived in the Appendix. Because the total density $\rho_{q=0}$ is a conserved quantity, we expect that $\lim_{q\to 0}\chi(q)$

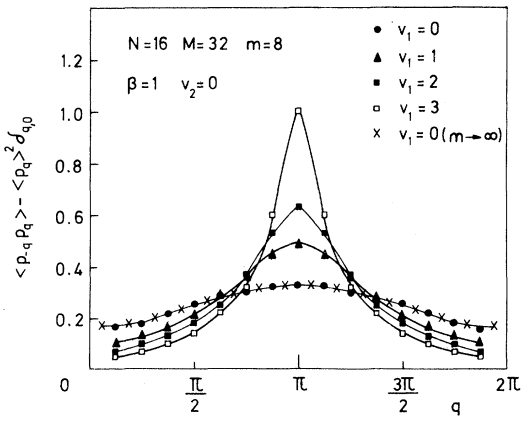

FIG. 1. Static structure factor at intermediate temperature for several values of $V(1)$. The crosses represent the exact result of the free-fermion model. Solid lines are guides for the eyes only.

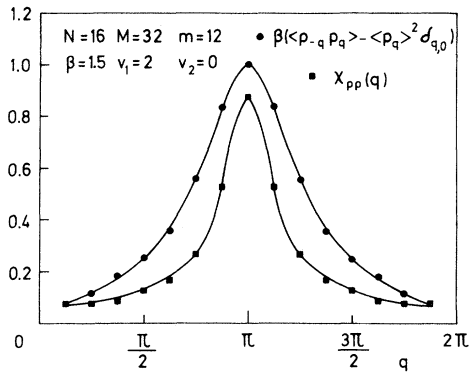

FIG. 2. Comparison between $\beta S(q)$ and $\chi(q)$ in the Heisenberg limit [$V(1)=2$, $V(2)=0$, $\rho=\frac{1}{2}$]. Solid lines are guides for the eyes only.

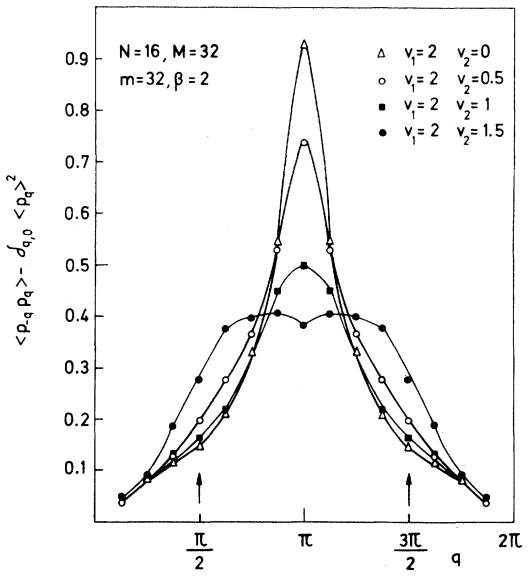

FIG. 3. Effect of the next-nearest-neighbor interaction on $S(q)$. The arrows indicate the peak position obtained in the classical limit ($t=0$) for $2V(2)>V(1)$. Solid lines are guides for the eyes only.

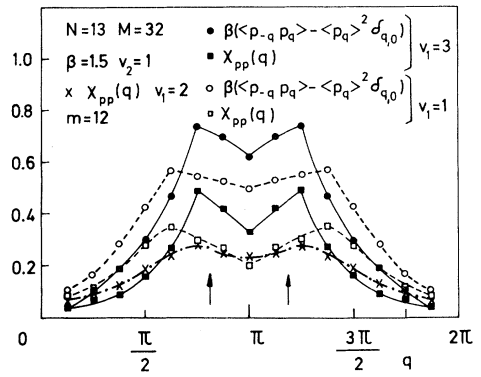

FIG. 4. $\chi(q)$ and $S(q)$ for $\rho=\frac{13}{32}$ for several values of $V(1)$. Note that the maxima in $\chi(q)$ are more pronounced. Solid lines are guides for the eyes only.

$=\beta \lim_{q\to 0} S(q)$, and this is indeed the case in our simulations. The effect of a nonzero next-nearest-neighbor interaction $V(2)$ on the system in the Heisenberg limit is shown in Fig. 3. First note that we have set $\beta=2$, corresponding to low temperature. We see that the maximum of $S(q)$ decreases rapidly as $V(2)$ approaches the critical value of the classical model $[V(2)\to 1]$, the shape of $S(q)$ remaining the same. If $V(2)>V(1)/2$, $S(q)$ broadens and it is difficult to determine the position of the maximum. In the classical limit ($t=0$) and at $T=0$, $S(q)$ diverges at $q=\pi/2,3\pi/2$ but the hopping term H_0 strongly mixes all possible states, leading to the broad structure observed in our simulations.

Let us now see what happens if we change the density ρ. In Fig. 4 we present $\beta S(q)$ and $\chi(q)$ for $\rho=\frac{13}{32}$, $V(2)=1$, and several values of $V(1)$. Again, we see immediately that the Bogoliubov inequality

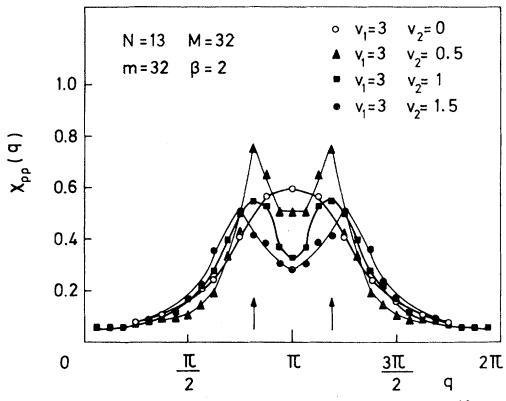

FIG. 5. $\chi(q)$ at low temperature for $\rho=\frac{13}{32}$. The nonzero bandwidth suppresses the maximum at $2k_F$. Solid lines are guides for the eyes only.

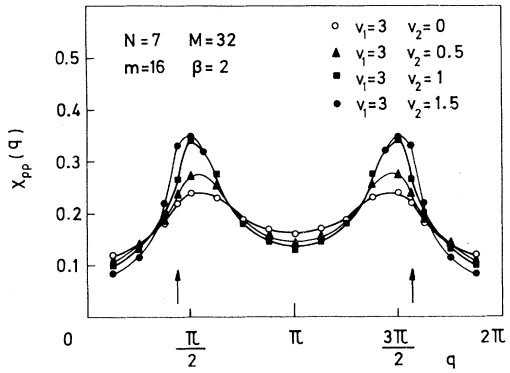

FIG. 6. $\chi(q)$ at low temperature and low density ($\rho=\frac{7}{32}$). Solid lines are guides for the eyes only.

is satisfied. The arrows indicate the position of the wave vectors $2k_F(=13\pi/16)$ and $2(\pi-k_F)$. It is clear that the $\beta S(q)$ and $\chi(q)$ have a maximum at these wave vectors and that the peaks are larger if $V(1)$ is greater than its Heisenberg model value $[V(1)=2]$. It is also striking that the peak structure in $\chi(q)$ is more pronounced than in $\beta S(q)$. Again, the hopping term H_0 wipes out most of the details of the classical Wigner lattice. For $V(2)<V(1)/2$, Hubbards algorithm for the ground state[1] gives the configuration

$$|\,10100101001010010100101001010100\rangle\ .$$

For this configuration $S(q)$ also peaks at $q=13\pi/32$ and $19\pi/32$.

If we go down in temperature, put $V(1)=3$, and vary $V(2)$, we obtain the results presented in Fig. 5. As before the arrows indicate the position of the maxima expected on the basis of a free-fermion or classical model. For $\rho=\frac{13}{32}$ and $V(2)=0$ there is some freedom for the particles to move without feeling each other through the nearest-neighbor interaction. This freedom seems to be enough to move the maximum to $q=\pi$. As soon as the next-nearest-neighbor interaction is turned on, this freedom is lost and $\chi(q)$ peaks in the neighborhood of the expected q values. If $V(2)$ approaches the critical value $V(2)=V(1)/2$, the relative maxima decrease and $\chi(q)$ smears out. This is consistent with the behavior for $\rho=\frac{1}{2}$ (see Fig. 3).

Finally Fig. 6 shows what happens for $\rho=\frac{7}{32}$. At this low density, a single-particle description should become useful and we might expect the Hartree-Fock approximation to work well. Indeed, we find maxima in $\chi(q)$ at the correct positions, and $S(q)$ (which is not shown) is flat for $2k_F<q<2(\pi-k_F)$.

IV. DISCUSSION

The spinless fermion Hamiltonian (1.1) is a simple model that might explain the $4k_F$ scattering in tetrathiofulvalene-tetracyanoquinodimethane (TTF-TCNQ).[13,14] Several different mechanisms to explain the observed scattering have been suggested.[1,15–19] All assume that there are strong repulsive interactions between the electrons. Usually the discussion starts from the extended Hubbard model[1,11]

$$H^e = -t\sum_{\sigma}\sum_{i=1}^{M}(a_{i,\sigma}^{\dagger}a_{i+1,\sigma}+a_{i+1,\sigma}^{\dagger}a_{i,\sigma}) + U\sum_{\sigma}\sum_{i=1}^{M}a_{i,\sigma}^{\dagger}a_{i,\sigma}a_{i,-\sigma}^{\dagger}a_{i,-\sigma} + \frac{1}{2}\sum_{\sigma,\sigma'}\sum_{i\neq j}^{M}V(|i-j|)a_{i,\sigma}^{\dagger}a_{i,\sigma}a_{j,\sigma'}^{\dagger}a_{j,\sigma'} .$$

In the limit of large on-site interaction U the electronic motion can be described by the spinless fermion model (1.1).[1,11,20] Then $4k_F^e$ in the electron model corresponds to $2k_F$ in the spinless model (1.1). Because the coupling to the lattice distortions has not been taken into account, one can interchange particles and holes such that $\rho\approx 0.6$ (which is the value of the charge transfer in TTF-TCNQ) is the same as $\rho\approx 0.4$. In this case, our simulations indicate that more-distant interactions are required to have a maximum at $4k_F^e$ in the spectral functions. Thus the Wigner lattice picture might explain the presence of $4k_F^e$ if more-distant interactions are strong. However, the hopping term H_0 redistributes the spectral weight in such a way that the relative maxima are not large. A qualitative measure of the effect of the nonzero bandwidth is obtained by comparing our figures with those of Ref. 8. We never observed the higher harmonics found in classical Monte Carlo work.[8]

A more complete picture can be obtained by taking electron-phonon interactions into account because it is via the lattice distortions that the $4k_F^e$ satellite is observed in x-ray scattering. If one makes the assumption that the coupling is linear in the lattice displacements, it is possible to eliminate the phonons analytically. We obtain a fermion model with retarded electron-electron interactions. From the point of view of simulations this only requires slight modifications in our program. Therefore, it is possible to apply the quantum Monte Carlo method to the electron-phonon model. We have shown that the Monte Carlo approach to quantum statistical mechanics can be useful to study model properties which are not accessible by current analytical methods.

ACKNOWLEDGMENTS

We would like to thank J. Fivez for helpful discussions and careful reading of the manuscript. This work is supported by the Belgian Interuniversitair Instituut voor Kernwetenschappen and the Dutch Stichting Fundamenteel Onderzoek der Materie.

APPENDIX

Here we derive an approximate expression for the static susceptibility

$$\chi_{AB} \equiv \int_0^{\beta} d\lambda \langle e^{\lambda H}A^{\dagger}e^{-\lambda H}B\rangle . \tag{A1}$$

Replacing the integral by a sum and application of the Trotter formula gives

$$\chi_{AB} \approx \frac{\tau}{Z_m}\sum_{j=1}^{m}\mathrm{Tr}(e^{-\tau H_0}e^{-\tau H_1})^{m-j} \times A^{\dagger}(e^{-\tau H_0}e^{-\tau H_1})^{j}B . \tag{A2}$$

If A and B are diagonal in the representation that diagonalizes the interaction H_1, we find (in the notation of Ref. 2)

$$\chi_{AB} \approx \tau\sum_{j=1}^{m}\frac{\langle\langle \mathrm{sgn}(P)A_{m-j+1}^{\dagger}B_1\rangle\rangle}{\langle\langle \mathrm{sgn}(P)\rangle\rangle} , \tag{A3}$$

where $A_j(B_j)$ denote the quantity measured on the jth chain. Using the cyclic permutation property of the trace, we can also write

$$\chi_{AB} \approx \frac{\tau}{m}\sum_{j=1}^{m}\sum_{j'=1}^{m}\frac{\langle\langle \mathrm{sgn}(P)A_j^{\dagger}B_{j'}\rangle\rangle}{\langle\langle \mathrm{sgn}(P)\rangle\rangle} . \tag{A4}$$

This quantity is expected to have statistical errors $1/\sqrt{m}$ times smaller than (A3), but because of the extra sum the computation time increases so drastically that we had to use (A3) in our simulation.

[1] J. Hubbard, Phys. Rev. B 17, 494 (1978).
[2] H. De Raedt and A. Lagendijk, Phys. Rev. Lett. 46, 77 (1981); J. Stat. Phys. 27, 731 (1982).
[3] M. Suzuki, S. Miyashita, and A. Kuroda, Prog. Theor. Phys. 58, 1377 (1977).
[4] J. E. Hirsch, D. J. Scalapino, R. L. Sugar, and R. Blankenbecler, Phys. Rev. Lett. 47, 1628 (1981).
[5] M. Fowler and M. W. Puga, Phys. Rev. B 18, 421 (1978).
[6] J. D. Johnson and B. M. McCoy, Phys. Rev. A 4, 1613

(1972); J. D. Johnson, S. Krinsky, and B. M. McCoy, *ibid.* 8, 2526 (1973); J. D. Johnson, *ibid.* 9, 1743 (1974).
[7]T. Schneider and E. Stoll, Phys. Rev. Lett. 47, 377 (1981).
[8]J. Kondo and K. Yamaji, J. Phys. Soc. Jpn. 43, 424 (1977).
[9]H. F. Trotter, Proc. Am. Math. Soc. 10, 545 (1959); M. Suzuki, Commun. Math. Phys. 51, 183 (1976).
[10]F. W. Wiegel, Phys. Rep. 16C, 2 (1975).
[11]V. J. Emery, in *Highly Conducting One-dimensional Solids,* edited by J. T. Devreese, R. P. Evrard, and V. E. van Doren (Plenum, New York, 1979).
[12]L. Hulthén, Ark. Mat. Astron. Fys. 26, 11 (1938).
[13]J. P. Pouget, S. K. Khanna, F. Denoyer, and R. Comès, Phys. Rev. Lett. 37, 437 (1976); S. Kagoshina, T. Ishiguru, and H. J. Anzai, J. Phys. Soc. Jpn. 41, 2061 (1976).
[14]J. P. Pouget, S. M. Shapiro, G. Shirane, A. F. Garito, and H. J. Heeger, Phys. Rev. B 19, 1792 (1979).
[15]J. B. Torrance, Phys. Rev. B 17, 3099 (1978).
[16]V. J. Emery, Phys. Rev. Lett. 37, 107 (1976).
[17]P. A. Lee, T. M. Rice, and P. A. Klemm, Phys. Rev. B 15, 2984 (1977).
[18]H. Sumi, Solid State Commun. 21, 17 (1977).
[19]S. Huizinga, J. Kommandeur, H. T. Jonkman, and C. Haas, Phys. Rev. B 25, 1717 (1982).
[20]A. A. Ovchinnikov, Zh. Eksp. Teor. Fiz. 64, 342 (1972) [Sov. Phys.—JETP 37, 176 (1973)].